Applied Catalysis B: Environmental 166–167 (2015) 592–602

Contents lists available at ScienceDirect

Applied Catalysis B: Environmental

journal homepage: www.elsevier.com/locate/apcatb

Review

Hydrocarbon adsorption and NO_x-SCR on (Cs,Co)mordenite

Ramiro M. Serra*, Soledad G. Aspromonte, Eduardo E. Miró, Alicia V. Boix

Instituto de Investigaciones en Catálisis y Petroquímica, INCAPE (FIQ, UNL-CONICET), Santiago del Estero 2829, 3000 Santa Fe, Argentina

ARTICLE INFO

Article history:
Received 25 May 2014
Received in revised form
17 November 2014
Accepted 28 November 2014
Available online 4 December 2014

Keywords:
Adsorption
Hydrocarbon traps
Toluene
Butane
Basicity

ABSTRACT

(Cs,Co)Mordenite catalysts with 2.9 wt.% of Co and either 2 or 7 wt.% of Cs are active for the selective reduction of NO_x with butane and toluene as reducing agents and, at the same time, they can act as hydrocarbon traps at the cold-start conditions of an engine. The presence of cesium does not decrease the catalytic activity of cobalt in the two reducing agents. When butane is the hydrocarbon, cesium increases the temperature window for NO_x reduction. The sulfur poisoning of the Cs_2CoM catalyst for the selective catalytic selective of NO_x with butane is investigated. The catalyst has medium sulfur tolerance and a lower tolerance to hydrothermal treatment. However, this catalyst showed a better performance against poisons compared with that of the CoM catalyst.

CoM has almost null adsorption capacity. The incorporation of a low amount of cesium (2 wt.%) notably enhances the adsorption properties and the toluene retention at temperatures higher than 100 °C. Probably, the presence of cesium increases the density charge of oxygen, so that it interacts more strongly with the C—H groups. In the samples studied, the adsorption capacity (μmoles m^{-2}) follows the order $Cs_2CoM \sim Cs_7CoM > NaM > CoM$ in both hydrocarbons. However, the desorption of butane occurs at temperatures significantly lower than that of toluene. This is related to the interaction of the C—H bonds (σ) that gives place to the interaction of butane with the zeolite structure through the hydrogen bridge bond (C—H···O). Additionally, in the case of toluene, the electronic interactions with the aromatic ring are very important.

When NO_x diluted in He is passed over the different catalysts with toluene adsorbed, the formation of isocyanate species takes place only when Co is present. These experiments also show that the hydrocarbon adsorption and the NO_x reduction may take place simultaneously over the Cs and Co sites, respectively.

Contents

* Corresponding author. Tel.: +54 03424536861.
E-mail address: rserra@fiq.unl.edu.ar (R.M. Serra).

http://dx.doi.org/10.1016/j.apcatb.2014.11.061
0926-3373/

1. Introduction

Emissions of nitrogen oxide (NO_x), carbon oxides (CO_x) and hydrocarbons (HCs) are responsible for different air pollution problems: they may affect human health since many of these compounds are toxic or even carcinogenic. A large variety of pollution sources has been identified, such as chemical and petrochemical industries and the use of fossil fuels, mainly natural gas and gasoline. It is known that over 50% of NO_x emissions are from automotive sources such as gasoline cars and diesel engine trucks, and over 40% of NO_x are from stationary sources such as power plants using fossil fuels [1].

At present, exhausts of gasoline vehicles are cleaned up by the use of three-way catalysts (TWC). These can work simultaneously and efficiently to reduce NO_x and oxidize COx and hydrocarbons at the theoretical air/fuel (A/F) ratio, ca. 14.6 [2]. However, TWC suffer from severe loss of activity for NO_x reduction in the presence of excess oxygen, which is the prevalent condition for lean-burn gasoline engines [3] and TWC are not active because the HCs are not present in the exhaust all the time. Thus, the selective catalytic reduction (SCR) of NO_x to N_2 represents a promising alternative and an important challenge for removing the NO_x emitted from diesel and lean-burn engines. It may provide a convenient and inexpensive process for the lean NO_x reduction using fuel or unburned hydrocarbons as reducing agents under lean burn conditions [4,5].

On the other hand, TWC are inactive at low temperatures, requiring values close to 300 °C for optimum performance. It has long been recognized that the key to reduce hydrocarbon emissions is to rapidly increase the temperature of the modern three-way catalysts when the vehicle is first started [6]. In this sense, the majority of HC emissions (up to 80%) occur during the cold-start period where any unburned HC is simply released from the tailpipe to the atmosphere [7–9].

The most common strategy regarding a potential solution to this problem is placing hydrocarbon traps before the TWC. First, hydrocarbons are trapped by adsorption in a porous material upstream of the catalytic converter; then, they are released when the catalyst has reached its working temperature and, consequently, they act as reducing agents for nitrogen oxides. However, the design of a catalyst which combines both processes might be a more promising route.

In addition, water vapor and sulfur dioxide are typically present in combustion exhausts and may cause a severe deactivation of catalysts for the SCR reaction and HC trap [10]. Usually, water vapor exists in the combustion exhaust of fuel varying with the air ratio [11]. Sulfur oxides (SO_x) are typically produced during the combustion of organic sulfur compounds, most of the SO_x being eluted as sulfur dioxide (SO_2). Thus, it is important for practical application that any catalyst be capable of retaining its activity in presence of both poisons.

For these processes, it is interesting to study materials with high surface and well-defined channel systems, as is the case of microporous solids. Molecular sieves such as zeolites are mainly used as catalysts or adsorbents due to their crystalline structure, high specific surface and thermodynamic affinity by different hydrocarbons [12]. Nonprotonic zeolites are employed in adsorption processes in order to avoid any catalytic transformation of the adsorbates on acid sites. The adsorption of a variety of hydrocarbons in zeolites has been studied and it has been established that the sorption properties depend on the number, strength, distribution and accessibility of adsorption sites and the framework topology. Many zeolites (such as FAU, MOR and BEA structures) in various alkali ion-exchanged forms have been described as adsorbents for practical applications and fundamental studies. In a previous work, we studied the theoretical and experimental behavior of the toluene adsorption on zeolites modified with different Cs and Na concentrations. We found that the main interaction of toluene takes place between the π electrons of the aromatic ring and the Lewis sites generated, and another interaction is between the C—H groups and the zeolite network oxygen [7,13].

On the other hand, zeolites can stabilize different cations as active sites for reactions like the oxidation of hydrocarbons and the reduction of nitrogen oxides, which are released in the combustion gases. Particularly, the catalysts based on cobalt-exchanged zeolites resulted active and selective in the conversion of *NO* to nitrogen with hydrocarbons [14–16].

It is noteworthy that this bimetallic material is a potential catalyst for diesel applications. Although the intrinsic activity of the catalysts is not enough to satisfy most emission standards, posses good behavior as hydrocarbon trap and good performance in SCR of the mobile sources, being sufficient for stationary sources.

Hence, the proposal suggested in this work has three main objectives: (i) investigate about the potential use of the solids in reducing HCs and NO_x emissions, (ii) study adsorption as a relevant step during the SCR reaction, and (iii) study hydrothermal aging and the influence of SO_2.

In this work, in order to combine catalytic and adsorbent properties, Cs cations were incorporated to Co-exchanged Na-mordenite catalysts in the structure. These catalysts were tested in the selective catalyst reduction of NO_x using butane or toluene as reducing agents. The selected HCs are representative of both the aliphatic and aromatic compounds which are present in the emission of vehicles. In addition, these solids were used as traps of toluene or butane at low temperature. The adsorption capacity and desorption temperature were also investigated. In addition, the effect of different poisons, water vapor or sulfur dioxide, was studied on the performance of the catalysts for the *SCR-NO* and toluene adsorption/desorption process. The thermal stability of adsorbed toluene and the reactivity with nitrogen monoxide were investigated by FTIR studies.

2. Experimental

2.1. Catalysts preparation

Commercial Na-mordenite (NaM) was used as parent zeolite (Si/Al = 6.5, $Na_{6.4}Al_{6.4}Si_{41.6}O_{96}(H_2O)_{24}$) [14]. The method used to incorporate cobalt and/or cesium in the zeolite support was ionic

exchange. The CoM sample with 2.9 wt.% of cobalt was prepared from 10 g of support mixed with 1 L of cobalt acetate solution (99.5 wt.%, Sigma–Aldrich) with a concentration of 0.05 M. The mixture was stirred during 24 h at 60 °C and afterwards it was filtered several times, washed and dried at 100 °C for 8 h. Then, the catalyst was calcined at 500 °C during 8 h on a stream of 25 $cm^3\ min^{-1}$ of air.

The bimetallic Cs_xCoM catalysts were prepared by a double ion exchange technique. First, the cobalt acetate was added following all the steps until obtaining the calcined CoM. Then, the second ion exchange was performed using cesium acetate solution (99.5 wt.%, Sigma–Aldrich). The cesium acetate concentration used was modified accordingly to obtain 2 and 7 wt.% of cesium. Then, all the materials were calcined in air flow at 500 °C and the content of Co and Cs incorporated to the NaM was determined by atomic absorption spectroscopy (AAS). The exchanged percentage was calculated used the unit cell and the metallic percentage obtained by AAS.

2.2. Characterization techniques

2.2.1. Textural properties

Nitrogen adsorption–desorption isotherms were obtained at −196 °C on a Quantachrome Autosorb instrument. Previously, samples were outgassed at 250 °C for 4 h under vacuum. The Brunauer–Emmet–Teller (BET) equation was used to calculate the specific surface area of the materials from nitrogen adsorption isotherms. The pore volume was obtained using a *t*-plot method.

2.2.2. X-ray photoelectron spectroscopy (XPS)

XPS analyses were performed in a multi-technique system (SPECS) equipped with a dual Mg/Al X-ray source and a hemispherical PHOIBOS 150 analyzer operating in the fixed analyzer transmission (FAT) mode. The spectra were obtained with a pass energy of 30 eV; an Al Kα X-ray source was operated at 200 W and 12 kV. The working pressure in the analyzing chamber was less than 5.9×10^{-7} Pa. Spectra were acquired in the Al 2s, Al 2p, C 1s, O 1s, Cs 3d, Na 1s, Si 2p, Si 2s and Cs 4p regions. The C 1s peak at 284.6 eV of binding energy (BE) was taken as reference. All the peaks were fitted by a Gaussian–Lorentzian component wave-form after an inelastic (Shirley-type) background had been subtracted in order to calculate the surface atomic ratio.

2.2.3. Thermal gravimetric analysis

The thermal behavior of the catalyst was studied in a Metter Toledo TGA/SDTA 851 instrument. The weight changes of the catalyst (≈15 mg of the samples) were analyzed from 25 to 900 °C with a heating rate of 10 °C min^{-1} in air flow (40 ml min^{-1}).

2.3. Catalytic activity measurements

The performance of the catalysts in the SCR-NO_x with toluene or butane was evaluated in a continuous flow system equipped with a fixed-bed quartz reactor. The concentrations of gases were analyzed with an on-line Shimadzu GC-2014 gas chromatograph equipped with a thermal conductivity detector (TCD). Nitrogen and oxygen were separated with a Zeolite 5A molecular sieve column at 45 °C, while toluene was determined with a Bentona-34 molecular sieve column at 45 °C. In the case of butane, it was detected with a Porapak Q molecular sieve column at 45 °C.

The reaction mixture typically contained 1000 ppm NO, 500 ppm of butane or 286 ppm of toluene, in both cases with ratio C/N = 2; 2% O_2 and 2% H_2O (balanced He) with a gas hourly space velocity, GHSV = 20,000 h^{-1}. Conversion profiles were obtained by increasing the temperature in steps of 50 °C and monitoring concentrations during 60–90 min at each temperature.

2.4. Toluene or butane adsorption and temperature-programmed desorption

The adsorption and desorption experiments were carried out in a continuous flow system. The stream of mixture toluene/He was obtained by passing pure He through two connected saturators that contained liquid C7H8 (99.9%, Sigma Aldrich). The temperature of saturators was kept at 0 °C with an ice bath which allowed obtaining approximately 8000 ppm of toluene. The sample (ca. 100 mg) was placed in a tubular quartz reactor of ca. 5 mm i.d., which was placed inside an electrical furnace equipped with a temperature controller. Subsequently, the sample was dehydrated in an inert flow at 500 °C for about 6 h. After cooling the solid sample to 100 °C, it was exposed to flow of C_7H_8/He during 1 h before the TPD experiments. In addition, the butane adsorption at 100 °C was studied using a flow of 25 ml min^{-1} of butane as adsorbate with a concentration of 10,000 ppm. Before the TPD experiments, a sweep under He flow at 100 °C was carried out. The temperature-programmed desorption was performed from 100 to 500 °C with a rate of 5 °C min^{-1} and maintaining it at the final temperature for about 10 min. The effluent gases were continuously monitored by on-line mass spectrometry (Pfeiffer/Balzers Quadstar, QMI422, QME125). The toluene concentration (m/e = 91) and the signal m/e = 43 which corresponds to the main partition of butane were registered through mass spectrometry. In addition, several other signals as 2 (hydrogen), 4 (helium), 28 (nitrogen or CO), 32 (oxygen), 105 (benzoic acid), 44 (CO_2), 77 (phenyl), 18 (water), 62 (pentene), 15 (methyl group) and 16 (methane) were monitored.

A typical breakthrough curve shows the evolution of the concentration of the hydrocarbon at the reactor outlet. The amount of hydrocarbon adsorbed during the breakthrough experiments (adsorption capacity) was calculated as the difference between the area under the curve in a blank experiment and the area under the breakthrough curve. The equation employed was:

$$Q_{ADS} = \frac{F}{W}\int_{t_1}^{\infty}(C_0 - C)dt \quad (1)$$

where Q_{ADS}: adsorbed hydrocarbon amount, F: flow adsorption, C_0: initial concentration of hydrocarbon, C: outlet hydrocarbon concentration, W: mass of catalyst.

We also measured the area under the curve during the TPD experiments, from which we can calculate the amount of toluene or butane desorbed between 100 and 550 °C. This amount corresponds to the toluene or butane that was retained in the sample after purging with He at 100 °C. Also we calculated the retention capacity (Φ = fraction of hydrocarbon desorbed at T > 100 °C).

2.5. Sulfur and water resistant test

In order to study the effect of SO_2 or H_2O over catalytic activity and adsorption performance, the Cs_2CoM and CoM catalysts were pretreated before the catalytic test and adsorption/desorption experiments. The sulfur pretreatment was 100 ppm SO_2 in air flow and was flowed for 8 h at 500 °C. After this treatment, the catalysts were purged with air for 2 h at the same temperature. The catalysts were also analyzed by the influence of water poison. In this sense, 2 wt.% of water vapor were introduced into the reactor at 500 °C during 8 h. After that, the catalyst was cooled in helium flow.

2.6. FTIR studies

FTIR spectra were collected with a Shimadzu 8101 M, model IR Prestige-21 equipped with DLATGS detector of high sensitivity. The adsorption measurements were made with 40 mg samples pressed into self-supported disks of approximately 1.3 cm in diameter and

Table 1
Chemical and textural properties of (Cs,Co)mordenite.

Samples[a]	% Exchange[b]	S_{BET}[c] ($m^2\ g^{-1}$)	Pore volume[d] ($cm^3\ g^{-1}$)
NaM	0	409	0.165
CoM	52	380	0.143
Cs_2CoM	62	338	0.129
Cs_7CoM	83	245	0.088

[a] The cobalt loading is 2.9 wt.% Co. The sub-index indicates the weight percentage of cesium.
[b] Percentage of ionic exchange of cobalt and cesium by sodium ions.
[c] Surface area calculated from N_2 isotherms at −196 °C.
[d] Micropore volume calculated by *t*-plot method.

placed in a sample holder at the center of the glass cell. The cell was equipped with $CaFl_2$ windows and it was heated externally. The temperature was measured by a thermocouple placed in the center near the sample. Absorption spectra were collected by recording 80 scans at a resolution of 4 cm^{-1}.

The sample was pretreated in inert flow at 400 °C for 4 h in order to remove adsorbed water. Then, the catalyst was cooled down to 100 °C. After recording a spectrum of the adsorbate free sample, the gas stream of ca. 8000 ppm of C_7H_8/He was passed through the cell for a period of about 1 h at 100 °C and atmospheric pressure. Subsequently, the cell was purged with He to remove all-gas-phase species, and then a spectrum was recorded. Then, the samples were heated in He, and the spectra were collected at different temperatures from 100 to 400 °C allowing a stabilization of 30 min before each measurement. Finally, the sample was purged overnight in He flow at 400 °C in order to know the stability of adsorbed toluene.

The stability and reactivity of the adsorbed species of toluene in the presence of an oxidizing gas such as nitrogen monoxide was also studied. To do this, the procedure was similar to the methodology described above, employing a stream of 1000 ppm of NO/He during the heating step.

3. Results and discussion

3.1. Chemical and textural properties

Table 1 shows the chemical and textural properties obtained for the NaM support and for the samples exchanged with cobalt or cobalt–cesium.

The surface area of NaM is in agreement with that reported by the zeolite supplier [17]. During the first exchange with cobalt acetate solution, 52% of Na^+ ions are replaced by Co^{2+} cations (Table 1) which are located at different sites inside of the structure. The specific surface area and the pore volume of CoM are slightly lower compared with the NaM support, indicating that the incorporation of cobalt and the dry and calcination treatments slightly modify the textural properties. However, when further bulky cations as cesium are introduced into the network, the surface area and pore volume decrease greatly.

3.2. Surface analysis

XPS measurements were performed to determine the chemical state and the relative abundance of surface species on the CoM and Cs_xCoM catalysts (calcined and after use in the SCR of NO_x with butane). The oxidation states of cesium and cobalt were determined by the deconvolution of the peaks corresponding to the region Cs 3d and Co 2p, respectively (Table 2).

In the monometallic CoM and bimetallic Cs_xCoM samples, the value of the binding energy of the Co $2p_{3/2}$ peak was between 781.3 and 781.6 eV, with a spin–orbit splitting between 797.3 and 797.6 eV corresponding to the Co $2p_{1/2}$ peak. The main peak was accompanied by a relatively intense 3d → 4s *shake-up* satellite peak between 786.9 and 787.2 eV, which is characteristic of the Co^{2+} species. Thus, these values are indicative of the presence of Co^{2+} in exchange position within the Na-mordenite. However, these binding energy values could also correspond to cobalt oxides (CoO, Co_3O_4). According to the results reported in our previous work, a fraction of dispersed cobalt oxides (22%) was detected in CoM by the temperature-programmed reduction technique (TPR) [15].

Table 2
Binding energies and surface concentration from XPS.

Samples[a]	Binding energy (eV) (FWHM)[b]		Surface ratio	
	Cs $3d_{5/2}$	Co $2p_{3/2}$	$(Cs/Si)_s$	$(Co/Si)_s$
CoM calc.	–	781.3 (4.6)	–	0.06
CoM us.	–	781.2 (4.0)	–	0.12
Cs_2CoM calc.	725.0 (2.3)	781.6 (4.5)	0.02	0.04
Cs_2CoM us.	725.0 (2.3)	781.6 (3.9)	0.02	0.04
Cs_7CoM calc.	725.1 (2.3)	781.5 (4.9)	0.03	0.05
Cs_7CoM us.	725.2 (2.3)	781.5 (5.1)	0.03	0.06

[a] Calc: calcined in air flow at 500 °C; us: used in the SCR-NO_x with butane as reducing agent.
[b] Full width at half maximum (FWHM).

On the other hand, the more intense XPS signal for cesium corresponded to the 3d electronic level, which presented a characteristic doublet $3d_{3/2}$–$3d_{5/2}$ with a spacing of 6 eV. The binding energy values measured for the Cs $3d_{5/2}$ peak were 725.0 and 725.1 eV for the Cs_xCoM, with 2 and 7 wt.% Cs (see Table 2). Thus, no significant changes were observed due to the presence of 2.9 wt.% Co because the energy binding by Cs_7M monometallic was 725.1 eV. Further, the binding energies of Si 2p and Al 2p core level spectra for all samples were 102.4 and 74.1 eV, respectively.

In addition, Table 2 presents the surface Co/Si and Cs/Si ratios, calculated from XPS, which were similar to the volumetric values (Co/Si = 0.04, Cs/Si = 0.02 (Cs_2CoM); Cs/Si = 0.05 (Cs_7CoM) suggesting a homogeneous distribution of the species in the support.

The CoM and Cs_xCoM catalysts showed similar binding energy values after use under reaction conditions. Thus, the cobalt and cesium cationic centers in the mordenite structure were not modified by the action of the reaction gases. Only the monometallic CoM catalyst showed a surface enrichment of cobalt promoted by reaction conditions.

3.3. Selective catalytic reduction using butane or toluene as reducing agent

Fig. 1 shows the NO to nitrogen conversion for the SCR in the presence of O_2 excess. The catalytic performance was studied in the absence and presence of 2% H_2O in the stream.

Under dry reaction conditions (Fig. 1A) using butane as reducing agent, the maximum conversions of NO to nitrogen were 48% and 42% at 400 °C for Cs_2CoM and Cs_7CoM, respectively. These conversion values were slightly lower than the maximum conversion (51%) shown by the CoM catalyst [15]. Furthermore, in general, the conversion curves obtained for the Cs_xCoM catalysts were above the values obtained for the CoM catalyst, except for the maximum value. This was observed in all the temperature range analyzed.

On the other hand, when the reducing agent used was an aromatic hydrocarbon such as toluene, the NO conversion was less than 30% between 300 and 500 °C (Fig. 1A) for the CoM and Cs_xCoM catalysts. However, the NO_x conversion increased for all the catalysts at higher temperatures. The maximum NO to N_2 conversion was obtained for the CoM catalyst and it was close to 70% at 550 °C.

In all catalysts, the butane and toluene conversion increased with the temperature and reached the value of 100% at the maximum *NO* conversion.

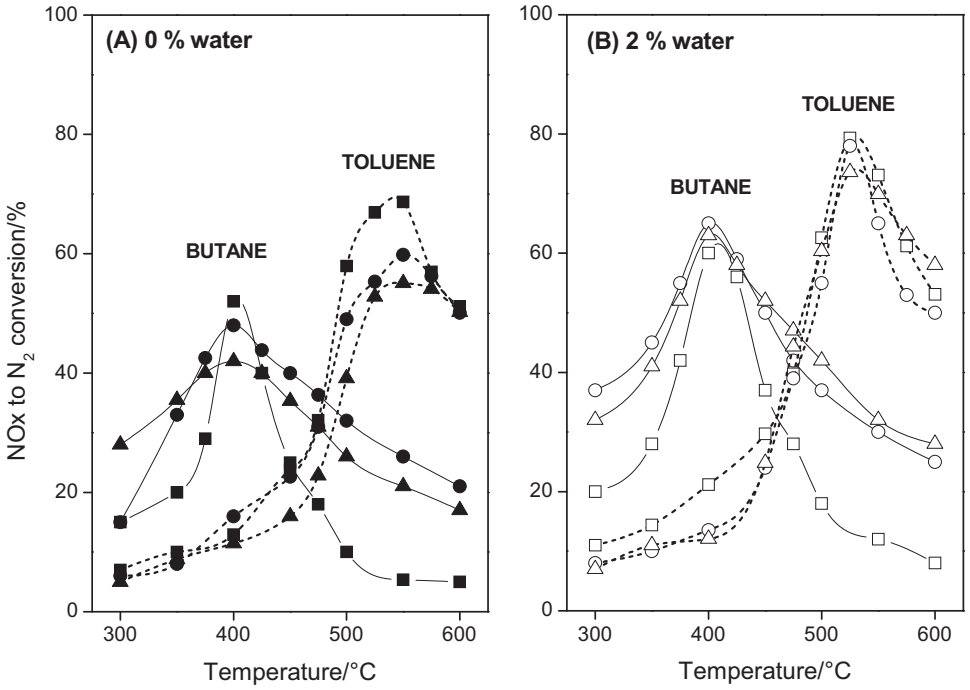

Fig. 1. The SCR of NO_x results obtained with toluene (dotted line) or butane (solid line) as reducing agents on Cs_xCoM catalysts: (■, □) 0 wt.% Cs (●, ○) 2 wt.% Cs; (▲, △) 7 wt.% Cs. Reaction conditions: GHSV = 20,000 h^{-1}, 1000 ppm NO, 2% O_2, 286 ppm C_7H_8 or 500 ppm C_4H_{10}, (A) dry or (B) wet (2% H_2O) conditions.

Besides, Fig. 1B shows the positive effect of adding 2 wt.% of water in the stream. The maximum NO conversion increased from 50% to values close to 60% using butane. In the same way, with toluene the NO conversions were greater than those under dry conditions. The CoM, Cs_2CoM and Cs_7CoM catalysts showed a similar catalytic behavior reaching a NO conversion c.a. 80% at higher temperatures. In a previous work, we studied the effect of water on the SCR-*NO* reaction [16]. The improvement of the NO conversion was attributed to a beneficial effect of water to maintain the surface clean from the carbon deposits.

Furthermore, it is important to note that an alkali metal, such as cesium, is not an active site for the SCR-*NO* using a hydrocarbon as reducing agent. This was confirmed from the catalytic evaluation of Cs-mordenite monometallic sample, which did not show catalytic activity. Therefore, the cobalt species, mainly Co^{2+} ions exchanged in the structure, are the active sites for the selective catalytic reduction of NO. After analyzing these results, it is observed that the addition of different contents of cesium to the CoM catalyst slightly affected the conversion obtained with the monometallic catalyst. This behavior was observed with butane or toluene under dry or wet conditions. Hence, it follows that the presence of a bulky metal such as cesium, does not interfere in the diffusion of the reactants to the active centers.

On the other hand, the analysis of the reducing activity of both hydrocarbons studied in this work is necessary. The SCR-*NO*, with butane or toluene reveals a similar behavior with some differences between them. Thus, it is very important to understand in general terms what happens during the process of NO_x reduction. A large number of studies conducted over Co-zeolites catalysts reported that the first step is the formation of NO_y ($y \geq 2$) at the active sites [18,19]. This process is carried out thorough the co-adsorption of NO and O_2 at Co^{2+} sites. In a second step, some authors reported that the NO_y groups could react chemically with the hydrocarbon molecule of the gas phase [14,20].

Other authors as Goryashenko et al. [21] also proposed the adsorption of hydrocarbon as a second stage. In this sense, these authors reported the IR spectra of surface species formed in $C_3H_6 + O_2$ co-adsorption on CoZSM5, and assigned spectral profiles to surface $C_kH_lO_m$ ($m \geq 0$) species. It was suggested that the second step of the reduction process is very likely due to the interaction between NO_y groups and $C_kH_lO_m$ ($m \geq 0$) species.

In our case, the main difference observed is that when toluene is used as reducing agent, the temperature of the maximum conversion is higher than with butane but the reaction mechanism of NO_x reduction appears to be similar for all the catalysts. The adsorbed NO reacts with O_2 and it is converted to NO_y groups at the active Co^{2+} sites. However, probably in the second stage different processes may occur simultaneously, namely, (i) the NO_y groups can react with gaseous butane or toluene, (ii) a possible interaction between the species present in the Cs_xCoM catalysts and the hydrocarbons, so that a fraction of NO_y groups would react with the adsorbed hydrocarbon, (iii) the decomposition of the HC at higher temperatures to produce hydrogen, which would promote the NO_x reduction. Therefore, it is important to study the interaction between hydrocarbons and the species present in the CsCoM catalysts.

As said above, in general the *NO* conversions are similar for CoM and CsCoM catalysts when the reducing agent is toluene. However, an interesting effect is observed for butane, consisting in a wider window for *NO* conversion when Cs is present. This effect could be related to the increase in adsorption capacity due to the alkali metal sites. When toluene is the hydrocarbon, despite that the active sites located inside of zeolite crystals are accessible to toluene molecules (as will be shown in the adsorption results), the reaction probably takes place preferentially at the outer surface of the mordenite crystals, to some extent due to diffusive limitation. Thus, the presence of Cs sites does not affect the catalytic activity. In the case of butane, a smaller straight-chain, the reaction may occur inside the zeolite channels. Thus, the adsorption on Cs sites may increase the concentration of butane molecules that surround the Co^{2+} active sites.

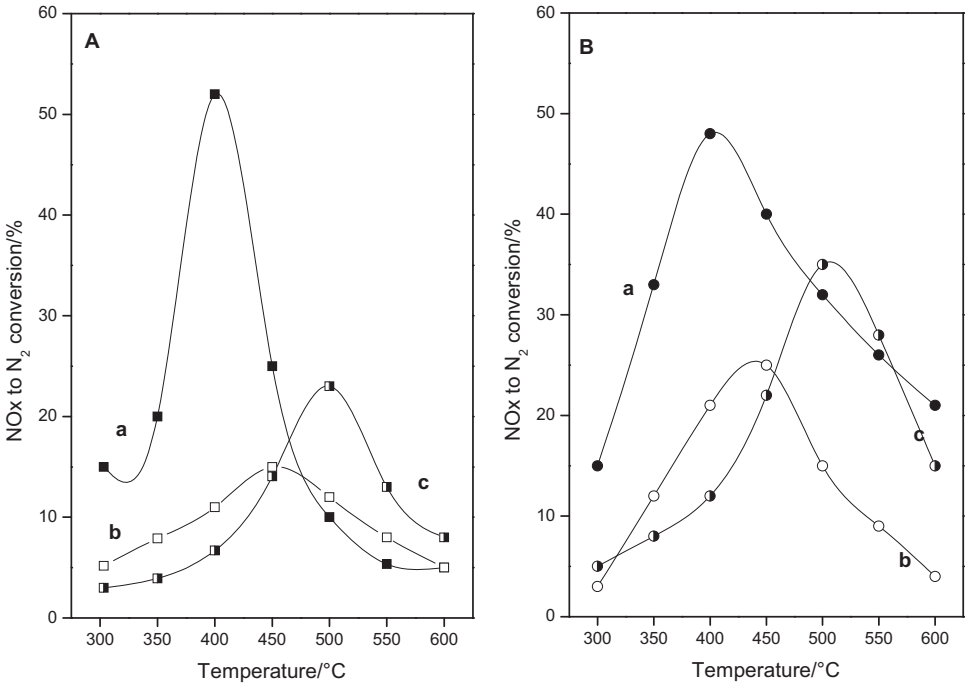

Fig. 2. SCR of NO by C_4H_{10} over (A) CoM and (B) Cs_2CoM. The samples were (a) calcined in air flow at 500 °C, (b) pretreated with 2% of water at 500 °C for 8 h and (c) pretreated with 100 ppm of SO_2 at 500 °C for 8 h. Conditions: GHSV = 20,000 h^{-1}, 2% O_2, C/N = 2.

3.4. *Effect of SO_2 or water vapor on the catalytic performance*

The most active CsCoM sample was chosen and compared to the monometallic CoM catalyst to study the hydrothermal ageing or SO_2 influence on the SCR-NO_x with butane.

Fig. 2 presents the catalytic behavior of the CoM and Cs_2CoM catalysts, which were pretreated with vapor water or SO_2 streams in order to study the effect of different poisons. In this sense, 100 ppm SO_2/air or 2% H_2O/He flow (50 cm^3 min^{-1}) flowed through the catalytic bed at 500 °C for 8 h.

The SCR-performance of the CoM and Cs_2CoM catalysts is shown in Fig. 2A and B, respectively, for the fresh-calcined (a), pre-steaming (b) and pre-SO_2 (c) samples. The NO conversion (Fig. 2A-b) for CoM significantly decreases from 51% to 15% after hydrothermal treatment. However, for Cs_2CoM the activity loss was attenuated by the presence of cesium. In addition, the temperature of the maximum *NO* conversion shifted from 400 °C (calcined catalyst) to 450 °C for the pre-steaming catalyst.

In contrast to the beneficial effect of 2% water co-fed with the reactants, which avoids the carbon deposition, the hydrothermal aging pretreatment irreversibly modifies the Co^{2+} active sites. It is known that water promotes the migration of cobalt ions and favors the formation of cobalt oxides. This species promotes the combustion of the hydrocarbons without the NO_x reduction taking place. However, the presence of cesium ions stabilized the cobalt ions into mordenite network minimizing the formation of inactive oxides.

The NO conversion curves of catalysts pretreated with SO_2 at 500 °C are shown below with respect to calcined solids. The maximun conversion decreases from 51% to 23% on CoM (Fig. 2A-c) and slightly less on *Cs_2CoM* (from 48% to 35%). Also, the temperature at the maximum conversion shifts to higher values, from 400 to 500 °C for the pre-SO_2 catalysts. In addition, it is worth noting that the poisoning by SO_2 was partially irreversible because, after the pretreatment with 100 ppm SO_2, the *NO* conversion was not recovered. It is known that the effect of sulfur dioxide over different Co species was different in the poisoning mechanism [22]. Probably, the presence of SO_2 produced the conversion of cobalt from isolated Co ions into cobalt oxides species and this process was irreversible. However, the presence of bulky molecules as cesium stabilizes the structure and prevents a fraction of the Co^{2+} ions active sites from coming into contact with sulfur dioxide thus allowing higher conversions.

Therefore, it is important to note that the incorporation of cesium on the CoM catalyst shows a similar activity for SCR-NO_x with hydrocarbons, and higher resistance to hydrothermal aging and poisoning by SO_2 than the conventional CoM catalyst. This result is very interesting in order to develop a catalyst able to work in the presence of water and sulfur compounds, which is important from an environmental point of view.

3.5. *Adsorption capacity of toluene and butane*

The evolution of the toluene or butane concentration, which was measured at the reactor outlet during the adsorption process, allowed the monitoring of adsorbent loading as a function of time.

Fig. 3 shows the adsorption breakthrough curves of CoM and Cs_xCoM catalysts measured at 100 °C. During the adsorption process, there is no signal at the reactor outlet ($C/C^o = 0$) for a short period which depends on the type of adsorbent. Table 3 shows that the adsorption capacity of toluene decreased considerably when 2.9 wt.% of cobalt were exchanged in the original Na-mordenite (Fig. 3A). However, when 2 wt.% of cesium were added to the CoM catalyst, the adsorption capacity was almost completely recovered. This is a positive effect that could be due to differences in the nature of the exchanged cation.

It is known that the sorption properties depend on the number, strength, distribution and accessibility of adsorption sites and the framework topology. The replacement of an atom (Si^{4+}) in a zeolite framework by another with a lower valency (Al^{3+}) creates a negative charge on the framework which has to be neutralized by a proton or a metal cation. Consequently, the conjugated acid–base pairs are then formed. The cation acts as a Lewis acid center, while the framework oxygen bearing partial negative charge behaves

Table 3
Toluene or butane adsorption capacity at 100 °C. Oxygen charge on Cs_xCoM catalysts.

Samples	Q_{ADS}^{TOL} (μmoles mg^{-1})	Q_{ADS}^{TOL} (μmoles m^{-2})	Q_{ADS}^{BUT} (μmoles mg^{-1})	Q_{ADS}^{BUT} (μmoles m^{-2})	$-\delta_{oxygen}$ [a]
CoM	0.33	0.87	0.09	0.24	0.1810
Cs_2CoM	1.31	3.87	0.29	0.86	0.1844
Cs_7CoM	0.87	3.55	0.22	0.90	0.2009
NaM	1.34	3.20	0.28	0.68	0.1985

[a] Zeolitic oxygen charge (calculated with Sanderson equation [23]). Q_{ADS} = adsorption capacity at 100 °C.

as a Lewis base center. For a given Al content, the acid character prevails for cations with a high electronegativity. However, when the framework negative charge is compensated by cations with a low electronegativity (like Na or Cs), the charge on the oxygen may be high enough to create basic properties. The charge on oxygen, expressing the basic strength, can be calculated theoretically according to Sanderson equation [23].

It has been proposed that the cations in zeolites are the adsorption sites for molecules with π electrons and numerous molecules of this type have been studied, particularly benzene. In this sense, the adsorption of toluene molecules involves the interaction through its π electron cloud with the cation and the interaction of the CH group with framework oxygens bearing the negative charge of the lattice [13].

Therefore, cobalt has two disadvantages to adsorb toluene compared with sodium or cesium. On the one hand, cobalt (2+) has a Sanderson electronegativity of 1.96, whereas sodium and cesium have electronegativities of 0.83 and 0.22, respectively [24]. This property decreases the charge density of the zeolite oxygen ($-\delta_{oxygen}$) (see Table 3) [7], and therefore has less interaction with the C—H groups of toluene and butane. In addition, a high content of Cs (7 wt.%) decreases the adsorption capacity of toluene. Thus, this lower adsorption capacity compared to Cs_2CoM is the result of a decrease of pore volume of the structure (Table 1). It can be clearly seen that, when the amounts of adsorbed toluene or butane are referred to the surface area, similar adsorption capacities are obtained (see column 3 in Table 3).

Fig. 3B shows the breakthrough curves obtained after butane adsorption at 100 °C on samples modified with Cs and Co. The amount of adsorbed butane at 100 °C is lower than toluene since the interaction of aliphatic hydrocarbon with the structure is weaker.

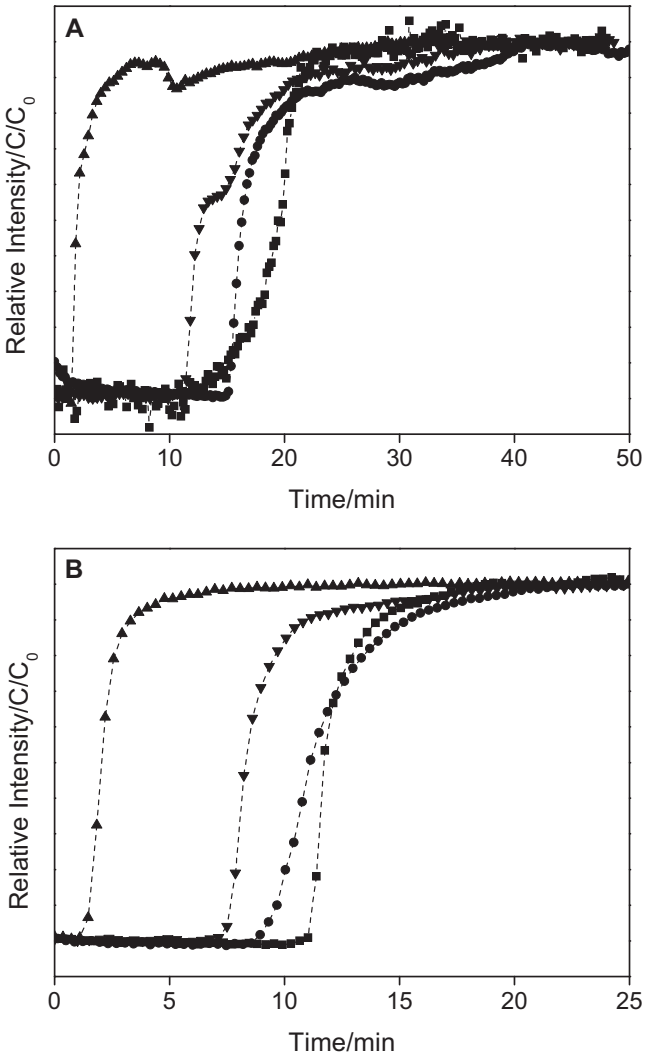

Fig. 3. Breakthrough curves corresponding to (A) toluene or (B) butane adsorption on (Cs,Co)mordenite catalysts: (■) NaM, (▲) 0 wt.% Cs, (●) 2 wt.% Cs, (▼) 7 wt.% Cs. Conditions: 100 mg of sample, 20 cm^3 min^{-1} and 8000 ppm toluene/He or 10,000 ppm butane/He.

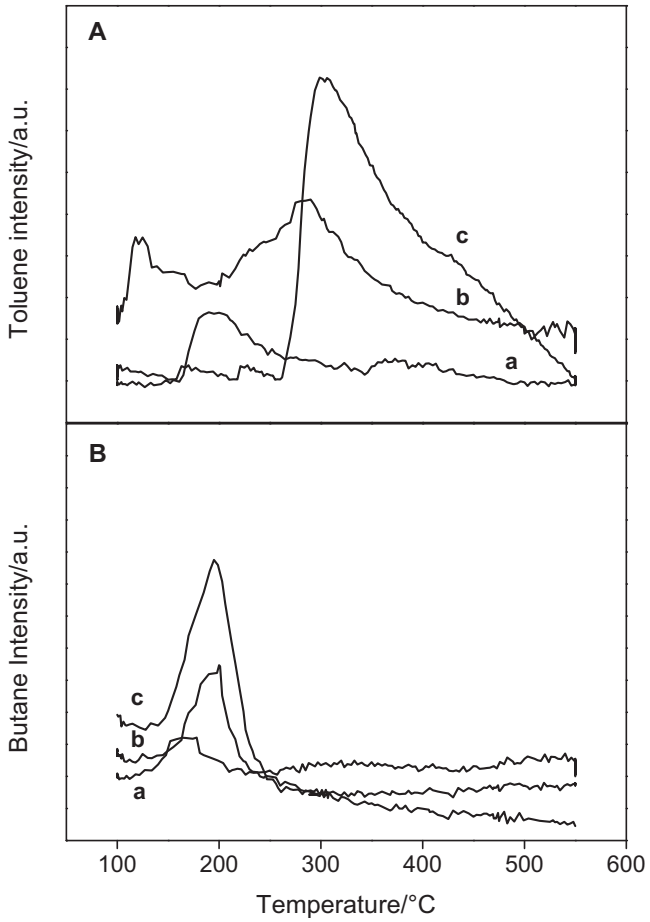

Fig. 4. Profiles of temperature-programmed desorption (TPD) of (A) adsorbed toluene or (B) butane at 100 °C. Desorption in He flow; heating rate 10 °C min^{-1}. Profiles: (a) CoM, (b) Cs_7CoM and (c) Cs_2CoM catalysts.

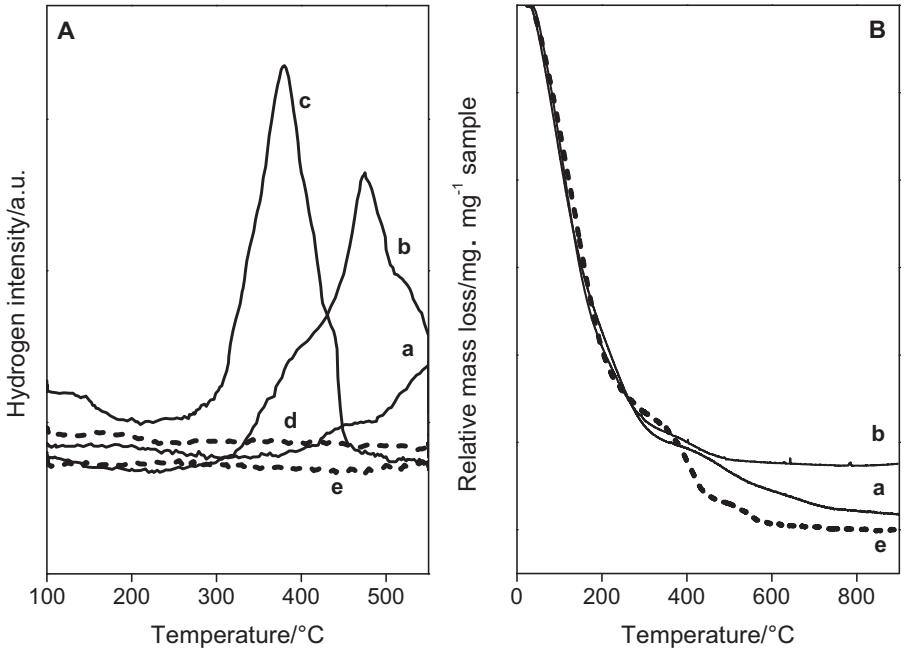

Fig. 5. (A) Profiles of temperature-programmed desorption (TPD) of H_2 after toluene adsorption at 100 °C. Desorption in He flow; heating rate 10 °C min^{-1}. (B) Thermal gravimetric analysis in air flow; heating rate 10 °C min^{-1}. (a) CoM, (b) Cs_7CoM, (c) Cs_2CoM, (d) NaM and (e) Cs_7M catalysts.

This effect could be due to the fact that butane has a unique way of interacting with the materials, trough the methyl group C—H and the oxygen of the mordenite.

When 2 and 7 wt.% of cesium were incorporated to the CoM sample (Table 3), the butane adsorption capacity was significantly recovered. As in the case of toluene adsorption (Fig. 3A), cesium provides the CoM catalyst with certain properties that reverse the negative effect of cobalt on the hydrocarbons adsorption process. Thus, the order of the butane adsorption capacity (μmoles m^{-2}) for the different samples was similar to that observed in toluene (Cs_2CoM ≈ Cs_7CoM > NaM > CoM).

Hence, the toluene adsorption involves the interaction through its π electron cloud with the cation (Lewis acid) and the interaction of the CH group with framework oxygens (Lewis base). In the case of butane only the interaction of CH groups with the Lewis base takes place, thus obtaining lower adsorption values as compared with toluene.

3.6. Retention capacity of toluene or butane

Fig. 4 shows the desorption profiles of toluene (Fig. 4A) or butane (Fig. 4B) chemisorbed on the Na-mordenite sample modified with Co^{2+} and Cs^+ cations.

The profile of desorption of toluene for the monometallic CoM catalyst (Fig. 4A) shows a single peak at 195 °C that could be associated with weakly adsorbed toluene. Table 4 shows the amount of toluene retained, and it was observed that cobalt significantly reduces this value with respect to the unmodified support. As said above, this effect can be directly related to the higher electronegativity of cobalt compared with sodium, which decreases the oxygen charge density and the interaction with the hydrocarbon.

Table 4
Hydrocarbon retention capacity of Cs_xCoM.

Samples	Toluene		Butane	
	Q_{des}^{TOT}[a] (μmoles mg^{-1})	Φ^{TOL}[b]	Q_{des}^{BUT}[a] (μmoles mg^{-1})	Φ^{BUT}[b]
CoM	0.09	0.27	0.007	0.08
Cs_2CoM	0.37	0.31	0.052	0.18
Cs_7CoM	0.19	0.35	0.015	0.07
NaM	0.88	0.65	0.069	0.24

[a] Toluene or butane amount desorbed at temperatures above 100 °C.
[b] Toluene or butane retention capacity above 100 °C defined as $\Phi^{HC} = Q_{des}^{HC}/Q_{ads}^{HC}$.

Also, it was noted that the incorporation of a low content of cesium (2 wt.%) to CoM improved the toluene retention and significantly recovered the retention temperature. As in the previous case, this effect could be due to the presence of cesium, which increased the density charge of oxygen, so interacts more strongly with the C—H groups.

When 7 wt.% of cesium were added to CoM, a higher proportion of the adsorbed toluene was released at temperatures above the adsorption. In a previous work, we observed that the increase in Cs content led to an increase in the retention capacity of toluene (Φ^{TOL}), which was in agreement with the increase of the basicity of the material [7].

It was also observed that the toluene desorption profile obtained for the Cs_7CoM (Fig. 4A) has two characteristic zones, one at low temperature between 150 and 300 °C, and another between 300 and 500 °C. The region at lower temperature could be associated with weakly adsorbed toluene. Instead, the toluene released at higher temperatures is linked with the hydrocarbon that interacts more strongly with the structure. Sarshar et al. [12] reported that the toluene adsorbed on the NaZSM*12* zeolite was released in two different temperature zones, and claimed that the hydrocarbon desorbed at higher temperature interacts with strong acid sites. Serra et al. [7] observed that the toluene was desorbed from NaM in two stages, attributing the higher temperature peak to more strongly adsorbed toluene due to the presence of the Na^+ cations. Thus, the two desorption regions were associated with the interaction between the π electron clouds with the Lewis acid sites and also with the interaction of the CH group with framework oxygens bearing the negative charge of the lattice on cation sites, such as Na^+.

On the other hand, Fig. 4B presents the desorption profiles of butane adsorbed on Cs_xCoM catalysts. The profiles of the butane desorption of these samples showed a unique peak, which is related

with the only interaction of the C—H bonds (σ) with the zeolite structure through the hydrogen bridge bond (C—H···O) [25,26].

Table 4 shows that the addition of 2 wt.% of cesium to CoM, increased the retention capacity (Φ) of CoM. It was found that the presence of cesium helped to restore the electron density around the oxygen and thereby, increased the interaction with hydrocarbon.

On the other hand, during the programmed-temperature desorption in He flow, besides recording the signals corresponding to toluene and butane, other species (m/z = 2, 16, 28, 30, 44, etc.) were measured. The signal m/z = 2 corresponding to H_2 was observed only in Cs_2CoM and Cs_7CoM catalysts. This signal appeared during toluene desorption above 300 °C (Fig. 5A). In the CoM sample, the hydrogen signal was small and the temperature of retention was lower than 300 °C, which suggested that the interaction between the hydrocarbon and the species present in the catalyst was poor. However, the H_2 signal was more intense for the bimetallic catalysts. It could be due to the toluene decomposition at temperatures higher than 300 °C and generated by the presence of cobalt cations. It is important to note that the cobalt cations (Co^{2+}) are active for the SCR-NO_x at temperatures higher than 300 °C. In this vein, Aspromonte et al. [27] reported the toluene decomposition reaction on the Ag(X)-zeolite. Also, Awadallah et al. [28] studied the natural gas decomposition to hydrogen and carbon nanotubes using a commercial catalyst of Co-Mo/Al_2O_3.

Then toluene may crack producing coke and hydrogen, by means of the following reaction [29]:

$$C_7H_8 \rightarrow 7C(s) + 4H_2(g) \quad (2)$$

To corroborate the carbon deposits, a thermal gravimetric analysis was performed on samples with H_2 release after adsorbing toluene at 100 °C. Fig. 5B shows that the mass loss profiles between room temperature and 200 °C are coincident, which correspond with hydration water retained in the cavity of structure. After that, the mass of monometallic Cs_7M unchanged, while the mass loss is higher in Cs_7CoM than CoM, associated with the carbon deposit in these catalysts according to the reaction (Eq. (2)).

3.7. *Effect of water and sulfur on the adsorption/desorption properties*

The effect of the water or sulfur dioxide on the toluene adsorption and retention capacity of the catalysts is of great importance for environmental applications. This is because water and SO_2 are present in significant amounts in a typical exhaust emission from combustion processes and the competitive adsorption with hydrocarbons may block the active sites of the catalysts. Thus, the CoM and Cs_2CoM catalysts were pretreated with 2 wt.% H_2O or 100 ppm SO_2 during 8 h at 500 °C after being evaluated in the adsorption/desorption of toluene.

Fig. 6A shows the breakthrough curves obtained for the toluene adsorption over CoM and Cs_2CoM after calcinations and pretreatments with H_2O or SO_2. The temperature program desorption curves are also shown in Fig. 6B and C. The quantitative results obtained from the breaking curve are shown in Table 5.

In Fig. 6A, it can be observed that the hydrothermal treatment has a higher power-off of the catalysts *CoM* and *Cs_2CoM* compared with sulfur poisonings. Table 5 shows that the toluene adsorption capacity of *CoM* decreases from 0.33 to 0.15 (μmoles mg^{-1}), while in Cs_2CoM decreases from 0.87 to 0.65 μmoles mg^{-1}. If we also consider the effect of the loss of specific surface area, the toluene adsorption capacity of CoM decreases from 0.87 to 0.41 μmoles m^{-2}; while in Cs_2CoM it decreases from 3.87 to 2.05 μmoles m^{-2}, 53% and 47%, respectively. In two catalysts, SO_2 provokes a slight decrease of toluene adsorption capacity;

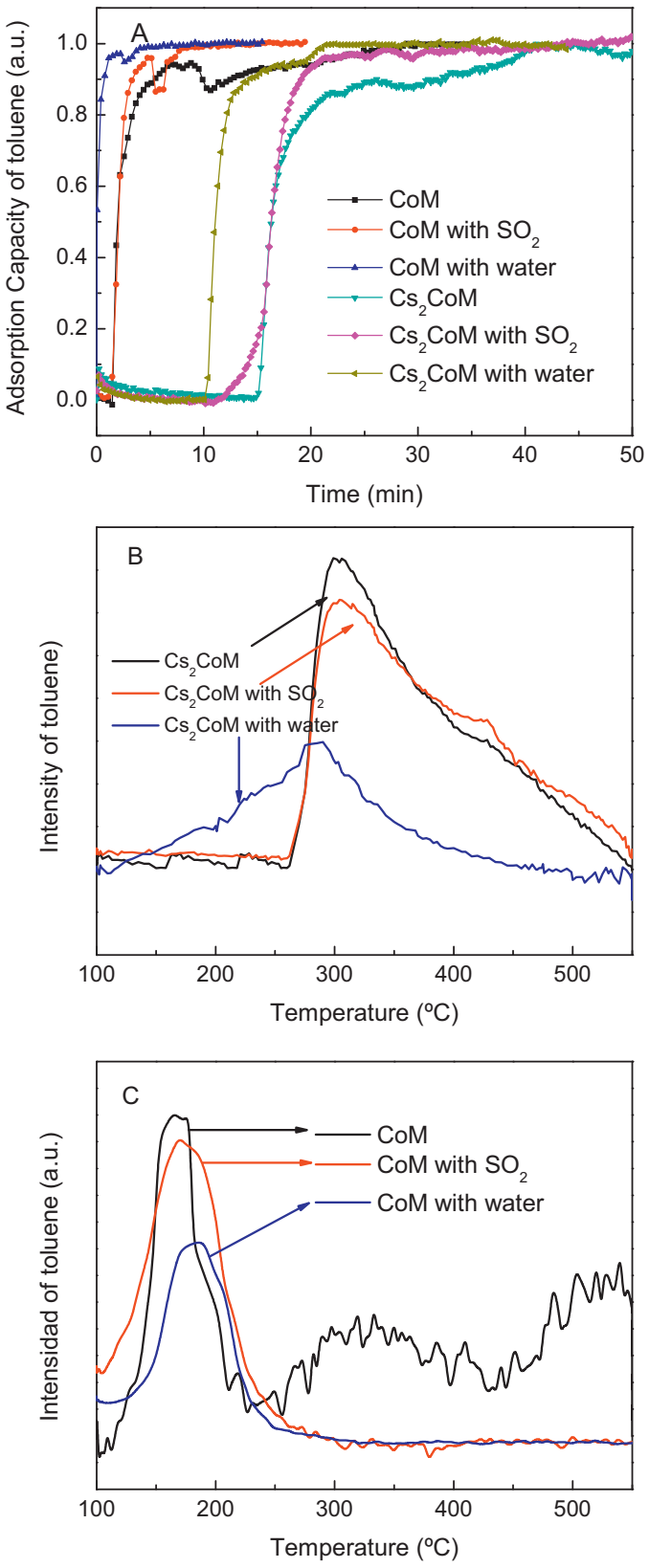

Fig. 6. (A) Breakthrough curves corresponding to *CoM and Cs_2CoM* after pretreated with 2 wt.% of water at 500 °C for 8 h or pretreated with 100 ppm of SO_2 at 500 °C for 8 h. (B and C) Profiles of toluene temperature-programmed desorption (TPD) after toluene adsorption at 100 °C on the samples *Cs_2CoM and CoM* pretreated with water or SO_2, respectively. Desorption in He flow; heating rate 10 °C min^{-1}.

Table 5
Effect of SO_2 or hydrothermal pretreatment on the toluene adsorption capacity of Cs_xCoM.

Pretreated samples	S_{BET} ($m^2\,g^{-1}$)	V_p ($cm^3\,g^{-1}$)	Q_{ADS} ($\mu mol\,mg^{-1}$)	Q_{des} ($\mu mol\,mg^{-1}$)	Φ^{TOL}
$CoM + SO_2$	351	0.131	0.29	0.09	0.31
$CoM + H_2O$	362	0.134	0.15	0.04	0.27
$Cs_2CoM + SO_2$	312	0.120	1.29	0.31	0.24
$Cs_2CoM + H_2O$	317	0.115	0.65	0.12	0.18

however, the hydrothermal treatments have a considerable effect on the toluene adsorption capacity.

Fig. 6B shows the toluene desorption profiles of the *Cs_2CoM* samples. In this case, it was observed that the aggregate of water provokes a shift in the temperature maximum. The SO_2 did not modify this temperature; however, the retention coefficient was modified (Table 5). The profiles of temperatures of the CoM sample were shown in Fig. 6C. In this case, both the maximum temperature desorption as retention capacity were not modified by the presence of poisons.

3.8. FTIR studies

Due to the potential use of these solids to remove hydrocarbons and nitrogen oxide simultaneously, the thermal stability of the species of toluene and nitrogen oxides adsorbed on Cs_2CoM catalyst was studied. This material was selected because it showed the best adsorption properties and high activity in the RCS.

The IR spectrum of toluene in the gas phase at 100 °C reported in the literature includes bands at 3099, 3034, 2925, 1614, 1506, 1465, 1450 and 1388 cm^{-1} [30]. The bands at 1614, 1506 and 1450 cm^{-1} correspond to the vibrational modes of the C=C stretching of the aromatic ring, while those shown at 1465 and 1388 cm^{-1} are assigned to the asymmetric and symmetric deformation that correspond to the methyl group. In a previous work, the thermal stability of toluene adsorbed in different zeolitic materials across the range of wavenumber was analyzed, whereas in this study only the spectral range at low wavenumber was analyzed [31].

The FTIR spectrums of adsorbed toluene shown in Fig. 7A and B were analyzed in a spectral bounded region between 1550 and 1300 cm^{-1}. In both regions, there appear bands at 1494 and 1450 cm^{-1}. The band that is located at 1494 cm^{-1} is the most intense one and corresponds to the C=C aromatic ring stretching mode. This band is displaced toward a lower wavenumber if compared to the corresponding gas phase toluene band (1506 cm^{-1}) when the hydrocarbon is adsorbed. Similar changes were previously studied in the case of benzene interacting with the OH group of zeolites [32]. This trend was also observed in a group of bands between 1515–1450 cm^{-1}, corresponding to C=C stretching. Lian Su et al. [33] attributed this shift to changes in electronic distribution and the symmetry of the aromatic ring when it interacts with the zeolite structure. Besides, a lower intensity band at 1450 cm^{-1} is observed in the spectrum, which corresponds to degenerate vibrations of the C=C bond of the aromatic ring [34].

Likewise, we can also see the appearance of the bands at 1465 and 1388 cm^{-1} assigned to the asymmetric and symmetric deformation of the methyl group, which disappear as the temperature increases. Aristizábal et al. [35] suggested that the weak band at 1388 cm^{-1} is associated with the interaction between the methyl group and Lewis acid sites.

Fig. 7B and C shows the spectra corresponding to the adsorption of toluene on Cs_2CoM, and a subsequent reaction with NO/He flow at different temperatures.

Fig. 7B shows a peak at 1494 cm^{-1}, corresponding to the aromatic ring C=C stretching of toluene. This peak remained in a presence of nitrogen oxides flow at different temperatures, which is positive effect because this HC could reduce the nitrogen oxides.

In addition, there appear two signals at 1460 and 1430 cm^{-1} which could be assigned to surface NO_2^- species (nitro, nitrite or nitro-nitrite form).

Fig. 7C shows a new band in the 2300–2050 cm^{-1} region, which corresponds to intermediate species produced by the

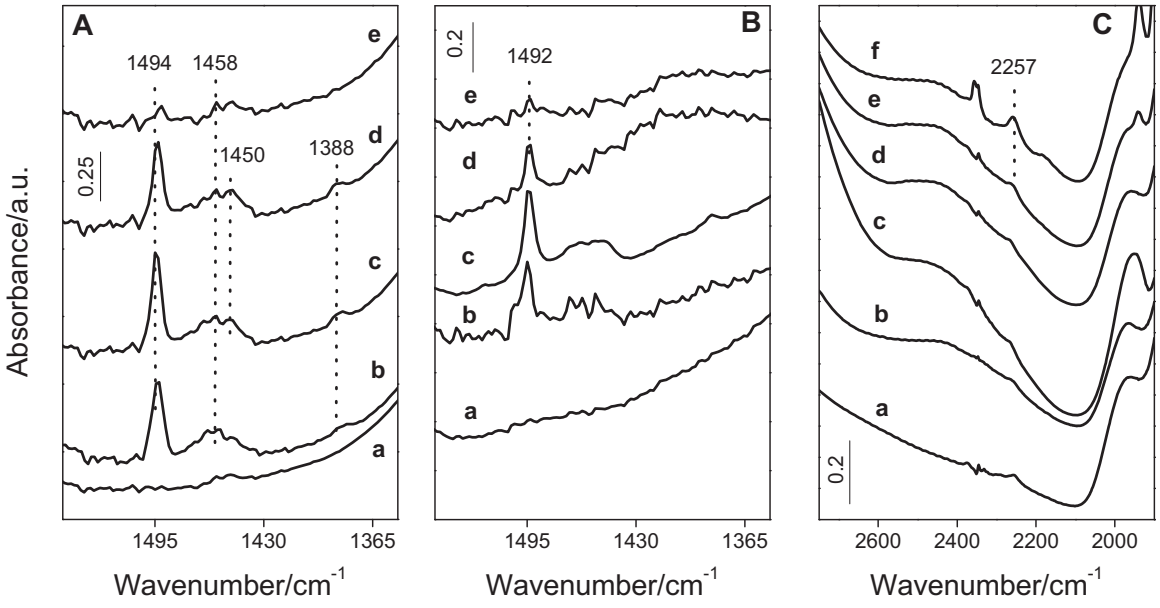

Fig. 7. FTIR of toluene adsorbed on dehydrated Cs_2CoM at different temperatures, (A) purged with N_2 flow, (B) and (C) purged with NO/He flow: spectrum (a) without toluene at 100 °C; (b) after toluene adsorption at 100 °C; (c) after heating at 100 °C; (d) 220 °C; (e) 330 °C; (f) 420 °C.

reaction between the adsorbed toluene and NO at 400 °C. The band at 2257 cm^{-1} is usually assigned to the stretching vibration of isocyanate groups (N═C═O) adsorbed on the catalyst surface [36].

However, through the analysis of FTIR spectra for the Cs_2CoM catalyst, it can be claimed that the adsorbed toluene shows characteristic vibrations of the C—H bonds of the methyl group and the C═C double bond of the aromatic ring. Toluene remains adsorbed up to 400 °C. When adsorbed toluene was swept with a NO/He mixture, intermediate species of the SCR of NO_x were observed. However, by sweeping with NO/He after adsorbing toluene, nitrate species were formed because the Cs^+ and Na^+ sites were occupied with toluene at the time of sweeping with NO/He. When we analyzed the material without cobalt, the signal corresponding to isocyanate was not observed; then, it could be assumed that cobalt is the cation active for SCR.

4. Conclusions

In this work, a novel solid is reported, which is active for the selective reduction of NO_x with butane and toluene as reducing agents and at the same time can act as a hydrocarbon trap during the engine cold start. The active component for the catalytic reaction is exchanged cobalt, while the cesium promotes the adsorption capacity. Another important result is that the presence of cesium in Cs_xCoM catalyst does not change the catalytic activity. Moreover, when butane is the reducing agent, cesium increases the temperature window for NO_x reduction.

With regard to adsorption properties, it is known that the parent sodium zeolite is effective for hydrocarbon adsorption. However, after Co exchange, the adsorption capacity is almost totally lost. The incorporation of a low amount of cesium (2 wt.%) restores the adsorption properties and significantly recovers the toluene retention at temperatures higher than 100 °C. This effect could be due to the presence of cesium, which increases the density charge of oxygen, therefore interacting more strongly with the C—H groups. Among the catalysts studied, the adsorption capacity (μmoles m^{-2}) follows the order $Cs_2CoM \sim Cs_7CoM > NaM > CoM$ for both hydrocarbons. The adsorbate butane interacts only through the C—H bonds (σ) with the zeolite structure through the hydrogen bridge bond (C—H···O).

CoM and Cs_2CoM were partially resistant to poisoning with water and sulfur dioxide. The study of SCR showed that the agreeing of cesium in *CoM* decreases the deactivation due to SO_2.

The formation of isocyanate intermediate was observed by FTIR when Co was present as the active component for the NO_x SCR. The hydrocarbons desorption and the NO_x reduction may take place simultaneously over Cs and Co sites, respectively.

Acknowledgments

The authors wish to acknowledge the financial support received from UNL, CONICET and ANPCyT. Thanks are given to Elsa Grimaldi for the English language editing and to Fernanda Mori for the XPS measurements.

References

[1] Q. Ye, L. Wang, R. Yang, Appl. Catal. A: Gen. 427–428 (2012) 24–34.
[2] M. Haneda, O. Houshito, T. Sato, H. Takagi, K. Shinoda, Y. Nakahara, K. Hiroe, H. Hamada, Catal. Commun. 11 (2010) 317–321.
[3] L. Landong, C. Jixin, Z. Shujuan, Z. Fuxiang, G. Naijia, W. Tianyou, L. Shuliang, Environ. Sci. Technol. 39 (2005) 2841–2847.
[4] J.M. García-Cortés, J. Pérez-Ramírez, M.J. Illán-Gómez, F. Kapteijn, J.A. Moulijn, C. Salinas-Martínez de Lecea, Appl. Catal. B: Environ. 30 (2001) 399–408.
[5] R.M. Serra, M.J. Vecchietti, E. Miró, A. Boix, Catal. Today 133–135 (2008) 480–486.
[6] S.P. Elangovan, M. Ogura, S. Ernst, M. Hartmann, S. Tontisirin, M.E. Davis, T. Okubo, Microporous Mesoporous. Mater. 96 (2006) 210–215.
[7] R.M. Serra, E.E. Miró, M.K. Sapag, A.V. Boix, Microporous Mesoporous. Mater. 138 (2011) 102–109.
[8] A. Iliyas, H.M. Zahedi-Niaki, M. Eíc, Appl. Catal. A: Gen. 382 (2010) 213–219.
[9] A. Westermann, B. Azambre, G. Finqueneisel, P. Da Costa, F. Can, Appl. Catal. B: Environ. 158–159 (2014) 48–59.
[10] Z. Li, M.F. Stephanopoulos, Appl. Catal. B: Environ. 22 (1999) 35–47.
[11] S.N. Orlyk, Catal. Today 191 (2012) 79–86.
[12] Z. Sarshar, M.H. Zahedi-Niaki, Q. Huang, M. Eic, S. Kaliaguine, Appl. Catal. B: Environ. 87 (2009) 37–45.
[13] R.M. Serra, P.G. Bolcatto, E.E. Miró, A.V. Boix, Microporous Mesoporous. Mater. 147 (2012) 17–29.
[14] F. Lóngy, H.E. Solt, J. Valyon, A. Boix, L.B. Gutierrez, Appl. Catal. B: Environ. 117–118 (2012) 212–223.
[15] A.V. Boix, S.G. Aspromonte, E.E. Miró, Appl. Catal. A: Gen. 341 (2008) 26–34.
[16] S.G. Aspromonte, E.E. Miró, A.V. Boix, Catal. Commun. 28 (2012) 105–110.
[17] Zeolyst International. Available from: http://www.zeolyst.com
[18] X. Wang, H. Chen, W. Sachtler, J. Catal. 197 (2001) 281–291.
[19] X. Chen, X. Yang, A. Zhu, C. Au, C. Shi, J. Mol. Catal. A: Chem. 312 (2009) 31–39.
[20] N. Cant, I. Liu, Catal. Today 63 (2000) 133–146.
[21] S.S. Goryashenko, Y. Park, D. Kim, S. Park, Res. Chem. Intermed. 24 (1998) 933–951.
[22] S. Chen, X. Yan, Y. Wang, J. Chen, D. Pan, Catal. Today 175 (2011) 12–17.
[23] R.T. Sanderson, J. Am. Chem. Soc. 105 (1983) 2259–2261.
[24] R.T. Sanderson, J. Chem. Educ. 65 (1988) 112–118.
[25] K. Czaplewski, T. Reitz, Y.J. Kim, R. Snurr, Microporous Mesoporous. Mater. 56 (2002) 55–64.
[26] M. Sánchez, T. Blanco, Catal. Today 143 (2009) 293–301.
[27] S.G. Aspromonte, R.M. Serra, E.E. Miró, A.V. Boix, Appl. Catal. A: Gen. 407 (2011) 134–144.
[28] A. Awadallah, A. Aboul-Enein, A. Aboul-Gheit, Energy Convers. Manage. 77 (2014) 143–151.
[29] E. Kantaris, P. Donaj, W. Yang, A. Zabaniotou, J. Hazard. Mater. 167 (2009) 675–684.
[30] C.J. Poucher, The Aldrich Library of Infrared spectra, 3rd ed., Aldrich Chemical Company, Wisconsin, USA, 1981.
[31] R.M. Serra, E.E. Miró, A.V. Boix, Microporous Mesoporous. Mater. 127 (2010) 182–189.
[32] B. Lian Su, V. Norberg, Colloids Surf. A: Physicochem. Eng. Aspects 187 (2001) 311–318.
[33] B. Lian Su, V. Norberg, J. Martens, Microporous Mesoporous. Mater. 25 (1998) 151–157.
[34] M. Larrubia, G. Busca, Appl. Catal. B: Environ. 39 (2002) 343–352.
[35] B.H. Aristizábal, C. Montes de Correa, A. Serykh, C. Hetrick, M. Amiridis, J. Catal. 258 (2008) 95–102.
[36] F. Dorado, A. De Lucas, P.B. García, A. Romero, J.L. Valverde, I. Asencio, Ind. Eng. Chem. Res. 44 (2005) 8988–8996.